Vol 14 No 10, October 2005
1009-1963/2005/14(10)/1974-10

Chinese Physics

© 2005 Chin. Phys. Soc.
and IOP Publishing Ltd

First-principle study of geometries, electronic structures and vibrational spectra of neutral and anionic onion-like $[As@Ni_{12}@As_{20}]^*$

Liu Hai-Tao(刘海涛)[a] and Li Jia-Ming(李家明)[b)a)c)†]

[a] *The Key Laboratory of Atomic and Molecular Nanosciences of the Ministry of Education, Department of Physics, Tsinghua University, Beijing* 100084, *China*

[b] *Department of Physics, Shanghai Jiao Tong University, Shanghai* 200030, *China*

[c] *Institute of Physics, Chinese Academy of Science, Beijing* 100080, *China*

(Received 27 April 2005; revised manuscript received 24 May 2005)

We present results of first-principle study for both neutral and anionic onion-like $[As@Ni_{12}@As_{20}]$. The ground-states of singly-charged and doubly-charged anions deviate from ideal I_h symmetrical geometry because of Jahn–Teller effect, whereas the triply-charged singlet and neutral quartet have similar stable geometries of I_h symmetry. The infrared and Raman spectra may provide a way to determine various charge states of this molecule with the same symmetry. Based on our systematical calculations, we suggest additional experimental measurements in order to determine the appropriate functional with great confidence, which should be important in the research for future quantum dot devices.

Keywords: clusters, density functional theory, first-principle calculation
PACC: 3640B, 3640C, 3220F

1. Introduction

Highly symmetrical molecules generally have special properties such as high stability and chemical inertness. They have been attracting much attention. In 1985, a football-like C_{60} molecule called buckminsterfullerene was first reported by Kroto *et al.*[1] Its I_h symmetry and stability indicated special properties for potential advanced materials. Recently, an I_h symmetrical carbon-free onion-like $[As@Ni_{12}@As_{20}]^{3-}$ anion has been prepared by Moses *et al.*[2] The structural parameters and properties have also been measured and investigated. Considering its high symmetry, some novel properties are expected to have applications as unit of nano-structured quantum devices with quantum dots. Therefore, it is interesting to carry out corresponding theoretical researches for such systems.

There have been some theoretical studies of such onion-like clusters. A semi-empirical extended Hückel molecular orbital (EHMO) calculation has been performed.[2] Since overlap integrals are fully or partially neglected in semi-empirical methods and artificial parameters are introduced, semi-empirical methods are greatly faster than first-principle methods. The calculated results from semi-empirical methods are fairly satisfactory especially for organic molecules. Semi-empirical methods can be used to explain their geometry structures, molecular vibrations, binding energy and even experimental spectra qualitatively. However, artificial parameters are neither flexible nor transferable because they are optimized for experimental values or high-level quantum chemistry calculations of a set of specific molecules. The first-principle methods do not depend on artificial parameters, and give accurate and highly transferable results. So it is very necessary to perform first-principle calculations for this system. Baruah *et al* have given a detailed first-principle study by adopting PBEPBE[3,4] functional for geometry, energetics, electronic structures, and vibrational properties for

*Project supported by the Ministry of Science and Technology (Grant No 2001CB610508), the Ministry of Education of China, and the National Natural Science Foundation of China (Grant No 10314010).

†E-mail: lijm@sjtu.edu.cn

both neutral and charged $[As@Ni_{12}@As_{20}]$ and its subunits, $[As_{20}]$ and $[As@Ni_{12}]$.[5] They have also studied the bonding scheme in the neutral $[As@Ni_{12}@As_{20}]$ and the energy barrier for removal of an arsenic atom from this neutral cluster. Zhao *et al*[6] have reported geometry, energetics, and electronic properties of the $[As@Ni_{12}@As_{20}]^{3-}$ anion, which adopted the PW91[7] functional with the plane-wave pseudopotential technique. They have also predicted the lower-energy absorption spectrum for this system by the time-dependent density functional theory. Because the exact energy functional is unknown, the comparison of validity and accuracy among various functionals is needed. In this article, both PBEPBE and other seven energy functionals are examined in the calculations of the triply-charged anion. All functionals lead to similar stable structures; particularly two hybrid functionals, i.e. B3PW91 and PBE1PBE are found to be the most suitable for this system. Some special techniques to reduce computational efforts are presented such as choices of basis sets and setting of algorithms because first-principle calculations are very time-consuming. We perform the geometry optimization and vibrational analysis with B3PW91 for the two stable I_h structures, i.e. the triply-charged singlet and the neutral quartet. Although their geometries are very similar, there are differences between their infrared (IR) and Raman spectra. It may provide a way to determine various charge states of this onion-like molecule with the same symmetry, which should be important in the research for future quantum dot devices.

2. Theoretical method and calculation results

Density functional theory (DFT)[8−10] has become more and more popular in recent years because of its successful balance of less computational requirement and adequate accuracy almost comparable with expensive post-SCF methods, such as, Møller-Plesset perturbation theory (MP),[11] configuration interaction (CI),[12−14] coupled-cluster (CC) method,[15,16] and complete-active-space multiple-configuration self-consistent-field method (CAS-MC-SCF).[17−20] Despite the great success in a wide range,[21,22] the exact functional is still unknown for the DFT method, so uncertainty to determine approximate energy functional exists in various specific applications. Before applying it to an unknown system, the validity and accuracy must be taken care of. More specifically, a more suitable functional for a given system must be chosen carefully from among lots of developed approximate functionals. The local density approximation (LDA) is simple, but very efficient and widely used for molecules, clusters and solid. But LDA has a general tendency to overbinding, i.e. contraction of bond length and overestimation of cohesive energy.[23] The generalized gradient approximation (GGA) introduces gradient correction and attempts to improve LDA results though overcorrection exists sometimes. Hybrid functional was initially suggested by Becke to mix a fraction of Hartree–Fock exchange into GGA functionals.[24] People found that hybrid functionals had often given better results of energetics, structures and properties. They even drew a conclusion that hybrid functionals was most accurate in the DFT methods,[25] although the computational effort of hybrid functionals was slightly more than LDA. All calculations reported here are performed by the Gaussian 03 suite of programs.[26] In this work, we perform comparisons among eight different functionals, i.e., SVWN, BLYP, BP86, PBEPBE, HCTH407,[27−29] B3LYP, B3PW91 and PBE1PBE. More specifically, SVWN is a popular LDA functional in Gaussian 03; BLYP, BP86, PBEPBE and HCTH407 are GGA functionals; B3LYP, B3PW91 and PBE1PBE are hybrid functionals. Note that the B3LYP and PBE1PBE are hybrid functionals based on the BLYP and PBEPBE, respectively. For example, the PBE1PBE exchange-correlation functional is given by the formula $E_{xc}^{\mathrm{PBE1PBE}} = \frac{1}{4}\left(E_x^{\mathrm{HF}} - E_x^{\mathrm{PBE}}\right) + E_{xc}^{\mathrm{PBE}}$,[30] where the E_x^{HF} is the Hartree–Fock exchange, the E_x^{PBE} is the PBE exchange functional, and the E_{xc}^{PBE} is the PBEPBE exchange-correlation functional, respectively.

Two standard types of all-electron and DFT-optimized basis sets in Gaussian 03 are chosen: a double-ζ valence plus polarization basis set (DGDZVP)[31,32] which is used earlier in another package DGauss, and a larger triple-ζ valence plus polarization basis set (TZVP).[33,34] For example, in the calculations of triply-charged $[As@Ni_{12}@As_{20}]^{3-}$ anion with the PBEPBE functional, very similar results are obtained for these two basis sets. More specifically, less than 0.001nm between optimized geometries, and only $4.2\mathrm{cm}^{-1}$ for the root mean square (RMS) error of vibrational frequencies. It shows that the DGDZVP is sufficient for the geometry optimization and vibra-

tional analysis. Moreover, additional single point calculation using TZVP at the geometrical structure determined with DGDZVP gives a HOMO–LUMO (the highest occupied molecular orbital and the lowest unoccupied molecular orbital) gap only 0.01eV below the TZVP optimized value. So we adopt DGDZVP for the geometry optimization and vibrational analysis, and TZVP for accurate properties such as energetics and HOMO–LUMO gap. For self-consistent field (SCF) calculation, tight convergence criterion less than 10^{-8} is adopted. The direct inversion in iterative subspace method (DIIS)[35] is used in order to accelerate SCF convergence. Since a grid-based integration scheme is used for the DFT calculation in Gaussian 03, a pruned (99,590) integration grid is used to reduce the error from numerical integration. Moreover, spin is restricted for a closed-shell triply-charge state, and unrestricted for other charge states. In the following sections, we will use the eight different functionals for calculations of geometry optimization, vibrational analysis, and electronic structures.

2.1. Geometry optimization

The Born-Oppenheimer approximation is used to separate the fast moving electrons from the slow moving nuclei. More specifically, the total wavefunction is written as $\Psi_{\text{total}}(\{\boldsymbol{R}\},\{\boldsymbol{r}\}) = \Psi_{\text{nuclei}}(\{\boldsymbol{R}\})\Psi_{\text{electrons}}(\{\boldsymbol{r}\};\{\boldsymbol{R}\})$, which means the nuclear and electronic motions are decoupled. The geometry optimization can be described as follow. With reasonable initial guessed coordinates, movement of electrons with fixed nuclear configuration is obtained by solving the Kohn–Sham (KS) equations.[9] Note that the shape of potential energy surface (PES) is good enough to compare with experimental or high-level post-SCF results despite of approximate energy functional.[36] Then, the forces on nuclei are calculated by Hellmann–Feynman theorem and the coordinates of nuclei are updated according to classic mechanics based on a given searching algorithm. With this process going on until given convergence criteria of forces and displacements are reached, a stationary point is obtained. For the accurate geometry, very tight convergence criteria of geometry optimization are used: the maximum and the RMS forces are less than 2×10^{-6} and 1×10^{-6} a.u., respectively; the maximum and the RMS displacements are less than 6×10^{-6} and 4×10^{-6} a.u., respectively. A frequency analysis can be performed to distinguish an equilibrium point from a saddle point, which will be elucidated in detail in the next subsection.

For large systems, the optimization strategy and initial calculation settings should be chosen carefully because of great computational efforts. It should be noted that final results are independent of the initial calculation settings. In our calculations, the Hellmann–Feynman forces are obtained with analytic derivatives, which are calculated by solving coupled-perturbed Kohn–Sham (CPKS) equations.[37,38] The analytic derivative is useful for both accuracy and saving computational effort. Moreover, the performance of the geometry optimization depends on the adopted coordinate system. Because the redundant internal coordinates are proved to be the most efficient,[39−41] we adopt the Berny algorithm with redundant internal coordinates[42] in our calculations. The point group symmetry is also important in the geometry optimization, which can be required for less computational effort, or neglected for exploring more degrees of freedom. Therefore we restrict $[\text{As@Ni}_{12}\text{@As}_{20}]^{3-}$ anion to experimental I_h symmetry, and vibrational analysis will be requested to validate this precondition.

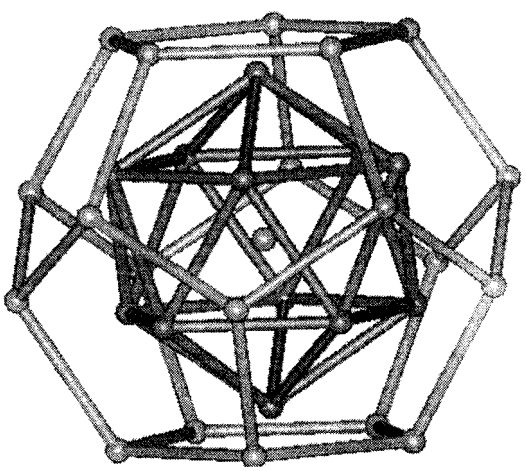


Fig.1. Structure of $[\text{As@Ni}_{12}\text{@As}_{20}]^{3-}$ anion.

The geometry of $[\text{As@Ni}_{12}\text{@As}_{20}]^{3-}$ can be illustrated as an three-shell onion-like structure as shown in Fig.1. More specifically, the outer-shell is a dodecahedral cage-like As_{20}, the intermediate-shell is a homocentric icosahedral cage-like Ni_{12}, and the inner arsenic atom is situated at their center. The experimental and theoretical structural parameters are depicted in Table 1. Note that the experiment is performed on crystal but the environmental effect on the triply-charged $[\text{As@Ni}_{12}\text{@As}_{20}]^{3-}$ is weak to be neglected,[2] thus the comparison between the experimental results and calculated values is reasonable.

It is shown that most DFT results are in reasonable agreement with the experimental results. For LDA results, the R_1, R_2, and R_3 accord with the experimental results within about 0.007nm. For GGA results, BLYP exhibits the greatest discrepancies within about 0.014nm, and the R_1, R_2 and R_3 of other GGA functionals are in accordance with the experimental results within about 0.005nm. For hybrid functionals, B3LYP results deviate less than 0.008nm from experimental results; B3PW91 and PBE1PBE results exhibit better agreements with the experimental results within about 0.003nm, which are also indicated by the ΔR in Table 1. The earlier first principle calculation results are also listed in Table 1. Their ΔR are larger than our B3PW91 and PBE1PBE results by a factor of three to five. Our PBEPBE results are close to Baruah's calculation,[5] which adopted the same functional and a bigger basis set.

Table 1. Structural parameters of $[As@Ni_{12}@As_{20}]^{3-}$ anion.

Functional	Type	R_1/0.1nm[a)]	R_2/0.1nm[b)]	R_3/0.1nm[c)]	ΔR/0.1nm[d)]
SVWN	LDA	2.73	2.49	2.39	0.041
BLYP	GGA	2.85	2.69	2.48	0.10
BP86	GGA	2.80	2.60	2.44	0.045
PBEPBE	GGA	2.79	2.58	2.44	0.036
HCTH407	GGA	2.77	2.54	2.42	0.020
B3LYP	Hybrid	2.80	2.63	2.44	0.055
B3PW91	Hybrid	2.77	2.56	2.41	0.012
PBE1PBE	Hybrid	2.75	2.53	2.40	0.014
PBEPBE, Baruah *et al*[5]	GGA	2.80	2.59	2.44	0.042
PW91,Zhao *et al*[6]	GGA	2.80	2.65	2.43	0.063
Exp.[2]		2.752 ± 0.025	2.558 ± 0.012	2.396 ± 0.008	0.000

a) R_1: the distances between two neighboring arsenic atoms of the As_{20} cage.
b) R_2: the distances between the central arsenic atom and a nickel atom.
c) R_3: the distances between a nickel atom and its neighboring arsenic atom of the As_{20} cage.
d) $\Delta R = \sqrt{\dfrac{(\Delta R_1)^2 + (\Delta R_2)^2 + (\Delta R_3)^2}{3}}$, $\Delta R_i = R_i - R_i^{\exp} \quad (i = 1, 2, 3)$.

2.2. Vibrational frequencies and spectra

The vibrational analysis is useful in determining whether the optimized structure is stable. The vibrational modes can be calculated by diagonalizing the mass-weighted Hessian matrix[43] based on the harmonic oscillator approximation. IR intensities[44] and Raman scattering activities[45] will be obtained by transforming the dipole derivative and polarizability derivative matrix to the normal coordinates respectively. Both Hessian matrix and the dipole derivative can be obtained analytically by solving CPKS equations but the polarizability derivatives have to be computed by numerical differentiation.

For I_h symmetrical $[As@Ni_{12}@As_{20}]^{3-}$ anion, the irreducible representation of vibrational structure is $\Gamma^{\mathrm{vib}} = 2A_g \oplus 1T_{1g} \oplus 1T_{2g} \oplus 3G_g \oplus 5H_g \oplus 4T_{1u} \oplus 3T_{2u} \oplus 3G_u \oplus 3H_u$. All computed vibrational frequencies are presented in Table 2. There is no imaginary frequency, which indicates that structures obtained by various functionals are all stable. All calculated frequencies are less than 330 cm^{-1}. Note that some imaginary frequencies are found in the Hartree–Fock (HF) calculation. As listed in Table 2, for most modes, the LDA type SVWN and the GGA type BLYP give the greatest and smallest frequencies respectively. For hybrid functionals, the B3PW91 and PBE1PBE results are mostly intermediate between the LDA and GGA results. It is interesting to note that there are extreme soft modes for BLYP and B3LYP (only 12.7 cm^{-1} and 7.4cm^{-1} for the lowest H_u mode, respectively). Our PBEPBE results are mostly in good agreement with Baruah's calculation[5] which is also listed in Table 2

Table 2. Vibrational frequencies of $[As@Ni_{12}@As_{20}]^{3-}$ anion (cm^{-1}).

Type	LDA	GGA					Hybrid		
	SVWN	BLYP	BP86	PBEPBE	PBEPBE[a)]	HCTH407	B3LYP	B3PW91	PBE1PBE
A_g	168.6	125.5	143.7	148.3	144	147.7	139.2	155.0	161.3
	247.3	201.4	220.6	226.1	227	230.3	220.4	238.0	246.4
T_{1g}	230.7	195.0	210.6	215.4	95	220.7	196.3	212.0	215.1
T_{2g}	97.6	83.5	90.0	92.2	222	96.1	89.7	95.7	98.0
G_g	104.6	72.7	86.5	90.0	89	90.4	73.6	87.9	91.4
	199.1	168.5	182.3	186.2	188	191.0	181.7	193.9	199.3
	276.9	229.9	250.1	256.0	258	259.4	243.0	261.2	267.8
H_g	87.3	51.6	69.3	74.3	72	78.8	56.9	73.4	78.1
	119.0	96.2	105.4	107.9	108	111.6	102.2	111.1	114.7
	142.5	114.2	126.3	129.4	131	129.0	122.8	134.1	138.7
	199.4	158.2	176.1	181.7	180	188.5	172.5	188.8	195.8
	316.7	262.6	285.6	291.8	295	294.3	280.8	301.3	309.4
T_{1u}	105.8	84.9	94.0	96.4	95	99.8	91.7	99.9	102.8
	225.1	144.5	182.9	194.1	187	205.2	161.3	195.8	207.7
	233.4	192.1	209.4	214.2	213	219.1	209.6	225.1	232.3
	286.9	239.5	259.6	265.1	269	268.3	253.9	271.9	278.6
T_{2u}	126.1	79.0	102.3	109.6	106	118.9	86.9	109.0	115.6
	146.2	119.3	129.2	131.9	135	131.8	124.3	133.6	137.3
	211.3	176.4	192.1	196.5	199	199.6	192.8	206.3	212.6
G_u	128.8	102.7	114.3	117.5	117	121.4	111.9	122.8	127.1
	157.7	130.9	142.7	146.4	147	152.8	142.8	153.5	158.4
	323.8	269.1	292.3	298.6	302	300.9	286.8	307.3	315.4
H_u	63.8	12.7	43.7	48.1	49	39.2	7.4	41.9	46.8
	104.6	78.5	89.3	92.7	96	92.1	86.9	97.3	102.0
	247.1	205.5	223.6	229.1	233	234.2	212.2	229.8	234.9

[a] Baruah's work, see Ref.[5].

Then we move on to considering IR intensities and Raman scattering activities, which are displayed in Table 3. The four T_{1u} modes are IR-active, together with two A_g and five H_g Raman-active modes. As shown in Table 3, the IR intensities and Raman scattering activities calculated by most functionals are consistent.

Table 3. IR intensities and Raman scattering activities of $[As@Ni_{12}@As_{20}]^{3-}$ anion.

Functional	Type	IR intensities/(km/mol)				Raman scattering activities/$((0.1nm)^4/amu)$						
		$1T_{1u}$	$2T_{1u}$	$3T_{1u}$	$4T_{1u}$	$1A_g$	$2A_g$	$1H_g$	$2H_g$	$3H_g$	$4H_g$	$5H_g$
SVWN	LDA	8.2	7.6	1.6	11.7	33.5	100.2	9.8	0.3	2.4	7.2	7.5
BLYP	GGA	9.1	1.1	7.1	6.3	24.0	124.5	8.7	1.8	3.1	8.8	11.3
BP86	GGA	8.4	2.5	6.1	8.7	28.8	116.3	9.4	0.9	2.9	8.4	9.8
PBEPBE	GGA	8.2	3.2	5.1	9.6	32.7	112.8	9.6	0.6	3.1	8.3	9.5
HCTH407	GGA	8.1	3.7	2.7	12.3	41.7	99.2	8.9	0.1	4.2	7.8	8.2
B3LYP	Hybrid	12.8	2.0	7.6	14.6	29.4	113.2	8.3	1.1	2.3	7.7	9.6
B3PW91	Hybrid	11.7	3.9	5.8	18.0	34.8	105.9	9.0	0.4	2.1	7.3	8.4
PBE1PBE	Hybrid	12.2	4.9	5.0	21.6	38.1	101.5	9.1	0.3	2.0	6.9	7.9

2.3. Electronic structures

The ground electronic state of $[As@Ni_{12}@As_{20}]^{3-}$ anion is a fully symmetrical ^1A_g. The order of computed molecular orbitals depends on the functional and the basis set. In our calculations, the LUMO is a fivefold degenerated h_g proposed by all function-

als. For the HOMO, SVWN, BP86, PBEPBE and HCTH407 give five-fold degenerated h_u, but BLYP, B3LYP, B3PW91 and PBE1PBE give a three-fold degenerated t_{1u}. All calculated HOMO–LUMO gaps are presented in Table 4. It shows that GGA and hybrid functionals give the smallest and greatest values, respectively. The hybrid functionals are anticipated to be better. The earlier first-principle calculation results are also listed in Table 4. Our PBEPBE results are in good agreement with Baruah's work,[5] and the HOMO–LUMO gap calculated by most GGA functionals is also in agreement with the Zhao's work.[6] Note that all earlier results predict that the HOMO is of h_u symmetry.

Table 4. Electronic configuration and HOMO–LUMO gap of $[As@Ni_{12}@As_{20}]^{3-}$ anion.

Functional	Type	Electronic configuration[a)]	HOMO–LUMO Gap/eV
SVWN	LDA	$(\cdots)(t_{2u})^6(h_g)^{10}(g_u)^8(g_g)^8(t_{1u})^6(a_g)^2(h_u)^{10}(h_g)^0(g_u)^0(t_{1u})^0(\cdots)$	1.58
BLYP	GGA	$(\cdots)(g_u)^8(t_{2u})^6(h_g)^{10}(a_g)^2(g_g)^8(h_u)^{10}(t_{1u})^6(h_g)^0(t_{1u})^0(g_u)^0(\cdots)$	1.33
BP86	GGA	$(\cdots)(g_u)^8(t_{2u})^6(h_g)^{10}(g_g)^8(a_g)^2(t_{1u})^6(h_u)^{10}(h_g)^0(t_{1u})^0(g_u)^0(\cdots)$	1.46
PBEPBE	GGA	$(\cdots)(t_{2u})^6(g_u)^8(h_g)^{10}(g_g)^8(a_g)^2(t_{1u})^6(h_u)^{10}(h_g)^0(g_u)^0(t_{1u})^0(\cdots)$	1.46
HCTH407	GGA	$(\cdots)(t_{2u})^6(h_g)^{10}(g_u)^8(g_g)^8(a_g)^2(t_{1u})^6(h_u)^{10}(h_g)^0(g_u)^0(t_{1u})^0(\cdots)$	1.55
B3LYP	Hybrid	$(\cdots)(t_{2u})^6(h_g)^{10}(g_u)^8(g_g)^8(a_g)^2(h_u)^{10}(t_{1u})^6(h_g)^0(t_{1u})^0(g_u)^0(\cdots)$	2.39
B3PW91	Hybrid	$(\cdots)(t_{2u})^6(h_g)^{10}(g_u)^8(g_g)^8(a_g)^2(h_u)^{10}(t_{1u})^6(h_g)^0(t_{1u})^0(g_u)^0(\cdots)$	2.54
PBE1PBE	Hybrid	$(\cdots)(t_{2u})^6(h_g)^{10}(g_u)^8(g_g)^8(a_g)^2(h_u)^{10}(t_{1u})^6(h_g)^0(t_{1u})^0(g_u)^0(\cdots)$	2.83
PBEPBE, Baruah *et al*[5]	GGA	$(\cdots)(t_{2u})^6(g_u)^8(h_g)^{10}(g_g)^8(a_g)^2(t_{1u})^6(h_u)^{10}(h_g)^0(\cdots)$	1.45
PW91, Zhao *et al*[6]	GGA	$(\cdots)(h_u)^{10}(g_u)^8(t_{1u})^6(h_g)^{10}(g_u)^8(g_g)^8(h_u)^{10}(h_g)^0(t_{1u})^0(g_u)^0(\cdots)$	1.44

a) Most closed shells are omitted in the representations of electronic configurations.

2.4. Polarizability

The mean polarizability of the $[As@Ni_{12}@As_{20}]^{3-}$ anion is listed in Table 5. The LDA type SVWN and the hybrid functional PBE1PBE give the smallest value, and the GGA type BLYP gives the greatest value. Most of our results are in the range from 25.1 to 26.6 bohr^3/atom which are in agreement with the PW91 results,[6] but our results are less than the PBEPBE result calculated by Baruah *et al.*[5] Note that the hybrid functional B3PW91 and PBE1PBE give consistent results.

Table 5. Mean polarizability of the $[As@Ni_{12}@As_{20}]^{3-}$ anion.

Functional	Type	Mean polarizability /(bohr^3/atom)
SVWN	LDA	25.1
BLYP	GGA	27.5
BP86	GGA	26.6
PBEPBE	GGA	26.4
HCTH407	GGA	25.5
B3LYP	Hybrid	26.1
B3PW91	Hybrid	25.4
PBE1PBE	Hybrid	25.1
PBEPBE, Baruah *et al*[5]	GGA	29
PW91,Zhao *et al*[6]	GGA	25.4

Based on above systematical calculations, the PBE1PBE and B3PW91 are found to be the most appropriate for the present physical system, which is consistent with available experimental measurements and theoretical results. Furthermore, in order to determine the appropriate functionals with great confidence, which should be important in the research for future quantum dots devices, we also suggest additional experimental measurements such as HOMO–LUMO gap, polarizability, IR and Raman spectroscopic measurements etc.

3. Discussion

As mentioned above, we have compared eight different functionals in the calculations for triply-charged $[As@Ni_{12}@As_{20}]^{3-}$ anion. As shown in Table 1 and Table 2, all calculated geometries of the onion-like I_h structure are stable and in agreement with the experimental results. The hybrid functionals, B3PW91 and PBE1PBE exhibit the best results. As shown in Table 4, the LUMO calculated by all eight functionals are h_g; For the HOMO, there are two predictions: one is predicted as t_{1u}, the other is as h_u. Although experimental measurements have not been performed yet, the hybrid functionals, B3PW91 and PBE1PBE are anticipated better; they predict the HOMO as t_{1u} and the HOMO–LUMO gaps as 2.54 and 2.83 eV, respectively. It deserves further exper-

imental measurements. A well-known drawback of LDA is the 'band gap problem',[46] which means that LDA underestimates the band gap generally, and for a finite system the band gap is corresponding to the HOMO–LUMO gap. This problem is even more severe for GGA because they give smaller HOMO–LUMO gaps than LDA in this work. The hybrid functionals are believed to meliorate the 'band gap problem' of LDA and GGA,[47−49] and show good agreement with more accurate theoretical values (for example, by the GW approximation,[50−52] and quantum Monte-Carlo method[53,54]) and experimental results.[55] In summary, hybrid functional B3PW91 and PBE1PBE are the most appropriate for this system. Furthermore, besides the HOMO–LUMO gap, we suggest additional experimental measurements such as polarizability, IR and Raman spectroscopic measurements etc., in order to determine the appropriate functionals with great confidence.

For the above discussion, we adopt only the B3PW91 in the following study for other charge states. According to the electronic configuration listed in Table 4, obtained by the hybrid functional B3PW91, the anticipated electronic configurations of various charge states are listed in Table 6. For I_h symmetry, the T_{1g}, T_{1u}, H_g and H_u states are unstable due to Jahn–Teller effect.[56] More specifically, the T_{1g} and T_{1u} electronic states interact with H_g vibrations, as well as the H_g and H_u electronic states interact with both G_g and H_g vibrations.[57,58] Therefore, the stable geometry of the ground states for the singly-charged and doubly-charged anions can not be of I_h symmetry. The stable geometries of the triply-charged singlet and neutral quartet are of I_h symmetry, because their electronic states are non-degenerated. The calculations of I_h structure of the neutral quartet will be reported below.

Table 6. Electronic states of anionic and neutral $[As@Ni_{12}@As_{20}]$.

Charge state	Electronic configuration	Electronic states
−3	$(\cdots)(t_{2u})^6(h_g)^{10}(g_u)^8(g_g)^8(a_g)^2(h_u)^{10}(t_{1u})^6$	^1A_g
−2	$(\cdots)(t_{2u})^6(h_g)^{10}(g_u)^8(g_g)^8(a_g)^2(h_u)^{10}(t_{1u})^5$	$^2T_{1u}$
−1	$(\cdots)(t_{2u})^6(h_g)^{10}(g_u)^8(g_g)^8(a_g)^2(h_u)^{10}(t_{1u})^4$	$^1A_g\oplus{}^1H_g\oplus{}^3T_{1g}$
0	$(\cdots)(t_{2u})^6(h_g)^{10}(g_u)^8(g_g)^8(a_g)^2(h_u)^{10}(t_{1u})^3$	$^2T_{1u}\oplus{}^2H_u\oplus{}^4A_u$

Some interesting results are shown in the comparison between the two optimized I_h equilibrium structures: the triply-charged singlet and the neutral quartet. They have very similar geometrical structures: As_{20} cage of neutral $[As@Ni_{12}@As_{20}]$ is nearly identical with the triply-charged anion, and Ni_{12} cage is less than 1% dilated for losing three electrons. The neutral species is 2.51eV energetically higher than the triply-charged anion, and has a 0.96eV HOMO–LUMO gap (which is defined as the smallest value of alpha and beta gaps), which is smaller than the 2.54eV gap of the triply-charged anion. For the neutral cluster, we find that the LUMO is of t_{1u} symmetry, which is in agreement with Baruah's calculation;[5] but the HOMO is of a_g symmetry instead of the h_u symmetry predicted by Baruah *et al.*[5] The mean polarizability of the neutral cluster is 24.9 $bohr^3$/atom, which is less than that of the triply-charged anion (25.4 $bohr^3$/atom). All vibrational frequencies of the triply-charged anion and the neutral cluster are listed in Table 7. Note that the two A_g and five H_g modes are Raman-active and the four T_{1u} modes are IR-active. Most of our calculated frequencies are similar to Baruah's result.[5] Note that for the lowest T_{1u} mode of the neutral species our result is 33 cm^{-1} less than Baruah's result.[5] For most modes, the differences in vibrational frequency between the triply-charged anion and neutral cluster are in agreement with Baruah's results,[5] as shown in Table 7. The IR and Raman spectra are shown in Fig.2. The Raman intensities are calculated by the method of Wojciechowski *et al.*[59] Note that our IR spectrum of the $[As@Ni_{12}@As_{20}]^{3-}$ anion is in agreement with the Baruah's result,[5] but the IR spectrum of the neutral $[As@Ni_{12}@As_{20}]$ cluster is different from their work.[5] Peak positions in our Raman spectra are in agreement with Baruah's work,[5] but the intensity distributions are different. It deserves further experimental measurements for verification, which should be important to determine the most appropriate functional for this system.

Based on our calculation results, the vibrational spectra may provide a way to determine various charge states of this molecule with the same symmetry. More specifically, for Raman spectra, vibrational frequen-

cies of all active modes are almost independent of charge states (within 6 cm^{-1}), as shown in Table 7. The intensity distributions in the range from 200 to 350 cm^{-1} are similar and there are some differences for soft modes, as shown in the Fig.2(c). For IR spectra, contrarily, the first, second and fourth IR-active T_{1u} modes are strongly red-shifted (by 48.2, 28.4 and 20.1 cm^{-1}, respectively) from triply-charged to neutral species, as shown in Table 7. The intensity distributions of IR spectra exhibit distinguishable differences between the triply-charged anion and the neutral cluster, as shown in Fig.2(d).

Table 7. Vibrational frequencies between triply-charged and neutral [As@Ni_{12}@As_{20}].

		Our work				Baruah's work[5]			
Mode		ν_{-3}/cm^{-1} a)	ν_0/cm^{-1} b)	$\Delta\nu/cm^{-1}$ c)	$(\Delta\nu/\nu)/\%$ d)	ν_{-3}/cm^{-1}	ν_0/cm^{-1}	$\Delta\nu/cm^{-1}$	$(\Delta\nu/\nu)/\%$
A_g	Raman	155.0	154.6	–0.4	–0.3	144	142	–2	–1.4
	Raman	238.0	236.2	–1.8	–0.8	227	227	0	0.0
T_{1g}		212.0	216.2	4.2	2.0	95	95	0	0.0
T_{2g}		95.7	93.6	–2.1	–2.2	222	222	0	0.0
G_g		87.9	79.9	–8.0	–9.1	89	87	–2	–2.2
		193.9	179.3	–14.6	–7.5	188	175	–13	–6.9
		261.2	266.1	4.9	1.9	258	265	7	2.7
H_g	Raman	73.4	67.7	–5.7	–7.8	72	67	–5	–6.9
	Raman	111.1	106.8	–4.3	–3.9	108	102	–6	–5.6
	Raman	134.1	136.3	2.2	1.6	131	130	–1	–0.8
	Raman	188.8	184.2	–4.6	–2.4	180	177	–3	–1.7
	Raman	301.3	301.3	0.0	0.0	295	297	2	0.7
T_{1u}	IR	99.9	51.7	–48.2	–48.2	95	85	–10	–10.5
	IR	195.8	167.4	–28.4	–14.5	187	163	–24	–12.8
	IR	225.1	219.2	–5.9	–2.6	213	212	–1	–0.5
	IR	271.9	251.8	–20.1	–7.4	269	265	–4	–1.5
T_{2u}		109.0	95.9	–13.1	–12.0	106	92	–14	–13.2
		133.6	121.1	–12.5	–9.4	135	128	–7	–5.2
		206.3	211.0	4.7	2.3	199	204	5	2.5
G_u		122.8	124.1	1.3	1.1	117	121	4	3.4
		153.5	143.6	–9.9	–6.4	147	140	–7	–4.8
		307.3	307.2	–0.1	0.0	302	305	3	1.0
H_u		41.9	32.3	–9.6	–22.9	49	43	–6	–12.2
		97.3	112.3	15.0	15.4	96	107	11	11.5
		229.8	234.4	4.6	2.0	233	238	5	2.1

a) ν_{-3}: vibrational frequencies of the triply-charged anion.
b) ν_0: vibrational frequencies of the neutral cluster.
c) $\Delta\nu = \nu_0 - \nu_{-3}$.
d) $\Delta\nu/\nu = (\nu_0 - \nu_{-3})/\nu_{-3}$.

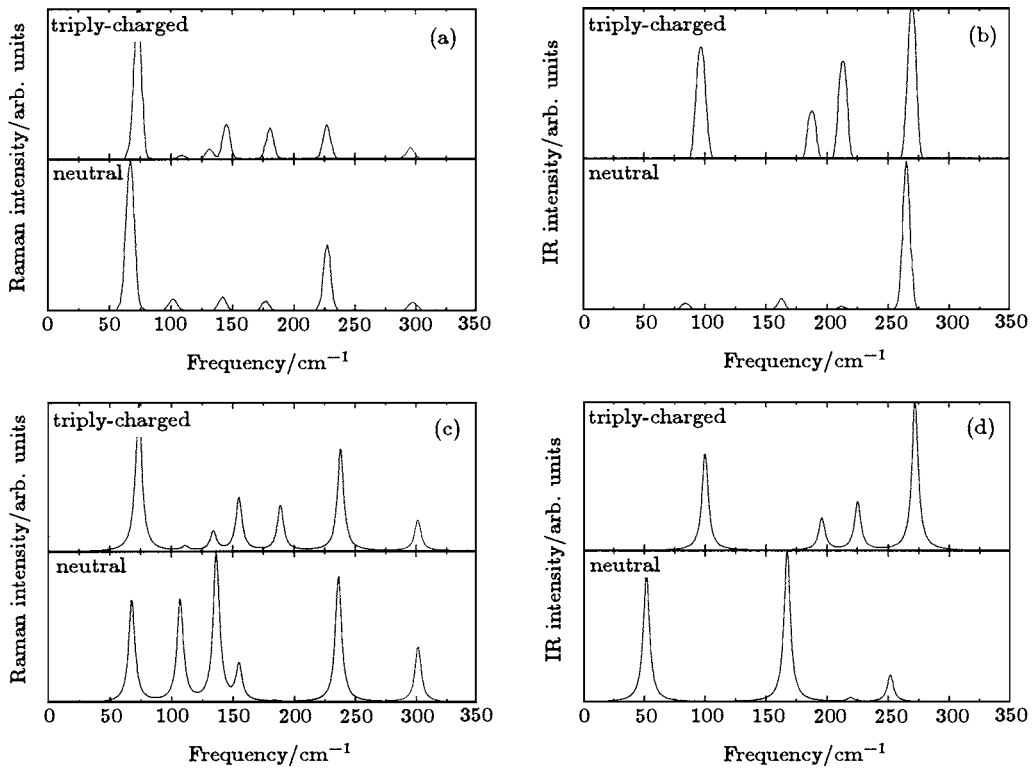


Fig.2. The Raman (a) and IR (b) spectra of both triply-charged and neutral [As@Ni_{12}@As_{20}] calculated by Baruah *et al*;[5] Our calculated Raman (c) and IR (d) spectra of both triply-charged and neutral [As@Ni_{12}@As_{20}].

Finally, we would like to conclude by making the following comments: It is important to examine functionals judiciously when we are going to study a cluster system. For the $[As@Ni_{12}@As_{20}]^{3-}$, the B3PW91 and PBE1PBE are determined to be the most appropriate. This onion-like system may be useful for future nano-structured quantum devices with quantum dots. The charge state of the quantum dots may be important for the functional performance. The IR and Raman spectra may provide a way to determine various charge states of this molecule with the same symmetry. Furthermore, based on our systematical calculations, we suggest additional experimental measurements in order to determine the appropriate functional with great confidence, which should be important in the research for future quantum dot devices.

References

[1] Kroto H W, Heath J R, O'Brien S C, Curl R F and Smalley R E 1985 *Nature* **318** 162

[2] Moses M J, Fettinger J C and Eichhorn B W 2003 *Science* **300** 778

[3] Perdew J P, Burke K and Ernzerhof M 1996 *Phys. Rev. Lett.* **77** 3865

[4] Perdew J P, Burke K and Ernzerhof M 1997 *Phys. Rev. Lett.* **78** 1396

[5] Baruah T, Zope R R, Richardson S L and Pederson M R 2003 *Phys. Rev.* B **68** (Rapid Communications) 241404(R) Baruah T, Zope R R, Richardson S L and Pederson M R 2004 *J. Chem. Phys.* **121** 11007

[6] Zhao J J and Xie R H 2004 *Chem. Phys. Lett.* **396** 161

[7] Perdew J P, Chevary J A, Vosko S H, Jackson K A, Pederson M R, Singh D J and Fiolhais C 1992 *Phys. Rev.* B **46** 6671

[8] Hohenberg P and Kohn W 1964 *Phys. Rev.* **136** B864

[9] Kohn W and Sham L J 1965 *Phys. Rev.* **140** A1133

[10] Parr R G and Yang W 1989 *Density-Functional Theory of Atoms and Molecules* (New York: Oxford University Press)

[11] Møller C and Plesset M S 1934 *Phys. Rev.* **46** 618

[12] Pople J A, Seeger R and Krishnan R 1977 *Int. J. Quant. Chem. Symp.* **11** 149

[13] Krishnan R, Schlegel H B and Pople J A 1980 *J. Chem. Phys.* **72** 4654

[14] Raghavachari K and Pople J A 1981 *Int. J. Quant Chem.* **20** 167

[15] Bartlett R B 1989 *J. Phys. Chem.* **93** 1697

[16] Lee T J and Scuseria G E, in S R Langhoff (ed.) 1995 *Quantum Mechanical Electronic Structure Calculations with Chemical Accuracy* (Dordrecht: Kluwer) p47-108

[17] Roos B O 1987 *Adv. Chem. Phys.* **69** 399

[18] Ruedenberg K, Cheung L M and Elbert S T 1979 *Int. J. Quant. Chem.* **16** 1069

[19] Roos B O and Taylor P R 1980 *Chem. Phys.* **48** 157

[20] Siegbahn P E M, Almlof J, Heiberg A and Roos B O 1981 *J. Chem. Phys.* **74** 2384
[21] Zheng HP and Hao J A 2005 *Chin. Phys.* **14** 529
[22] Tan M Q, Tao X M and Bao S N 2000 *Chin. Phys.* **9** 55
[23] Hafner J 2000 *Acta Mater.* **48** 71
[24] Becke A D 1993 *J. Chem. Phys.* **98** 5648
[25] Filatov M and Thiel W 1997 *Mol. Phys.* **91** 847
[26] Gaussian 03, Revision B.04, Frisch M J *et al* Gaussian, Inc., Pittsburgh PA, 2003
[27] Hamprecht F A, Cohen A J, Tozer D J and Handy N C 1998 *J. Chem. Phys.* **109** 6264
[28] Boese A D, Doltsinis N L, Handy N C and Sprik M 2000 *J. Chem. Phys.* **112** 1670
[29] Boese A D and Handy N C 2001 *J. Chem. Phys.* **114** 5497
[30] Ernzerhof M and Scuseria G E 1999 *J. Chem. Phys.* **110** 5029
[31] Godbout N, Salahub D R, Andzelm J and Wimmer E 1992 *Can. J. Chem.* **70** 560
[32] Sosa C, Andzelm J, Elkin B C, Wimmer E, Dobbs K D and Dixon D A 1992 *J. Phys. Chem.* **96** 6630
[33] Schaefer A, Horn H and Ahlrichs R 1992 *J. Chem. Phys.* **97** 2571
[34] Schaefer A, Huber C and Ahlrichs R 1994 *J. Chem. Phys.* **100** 5829
[35] Pulay P 1982 *J. Comput Chem.* **3** 556
[36] Xu R Q, Su C R, Xie J K and Li J M 2002 *Sci. China Ser.* A **45** 87
[37] Johnson B G and Frisch M J 1994 *J. Chem. Phys.* **100** 7429
[38] Stratmann R E, Burant J C, Scuseria G E and Frisch M J 1997 *J. Chem. Phys.* **106** 10175
[39] Pulay P, Fogarasi G, Pang F and Boggs J E 1979 *J. Am. Chem. Soc.* **101** 2550
[40] Pulay P and Fogarasi G 1992 *J. Chem. Phys.* **96** 2856
[41] Fogarasi G, Zhou X, Taylor P and Pulay P 1992 *J. Am. Chem. Soc.* **114** 8191
[42] Peng C, Ayala P Y, Schlegel H B and Frisch M J 1996 *J. Comp. Chem.* **17** 49
[43] Ochterski J W *Vibrational Analysis in Gaussian* p1 (technique notes of Gaussian Inc.)
[44] Yamaguchi Y, Frisch M J, Gaw J, Schaefer H F III and Binkley J S 1986 *J. Chem. Phys.* **84** 2262
[45] Frisch M J, Yamaguchi Y, Gaw Y F, Schaefer H F III and Binkley J S 1986 *J. Chem. Phys.* **84** 531
[46] Seidl A, Görling A, Vogl P, Majewski J A and Levy M 1996 *Phys. Rev.* B **53** 3764
[47] Salzner U, Pickup P G, Poirier R A and Lagowshi J B 1998 *J. Phys. Chem.* A **102** 2572
[48] Salzner U, Lagowski J B, Pickup P G and Poirier R A 1997 *J. Comp. Chem.* **18** 1943
[49] Koch W and Holthausen M C 2001 *A Chemist's Guide to Density Functional Theory* (Weinheim: Wiley-VCH)
[50] Hedin L 1965 *Phys. Rev.* **139** A796
[51] Hedin L and Lundqvist S 1969 *Solid State Physics, Advances in Research and Application*, edited by F Seitz, D Turnbell, and H Ehrenreich (New York: Academic) Vol 23 p1.
[52] Rohlfing M and Louie S G 1998 *Phys. Rev. Lett.* **80** 3320
[53] Anderson J B 1999 *Rev. Comput. Chem.* **13** 132
[54] Lester W A and Barett R N 1998 *Encycl. Comput. Chem.* **3** 1735
[55] Martin R M 2004 *Electronic Structure: Basic Theory and Practical Methods* (Cambridge University Press) p304
[56] Jahn H A and Teller E 1937 *Proc. Roy. Soc.* A **161** 220
[57] Herzberg G 1966 *Molecular Spectra and Molecular Structure, III. Electronic Spectra and Electronic Structure of Polyatomic Molecules* (New York: Van Nostrand Reinhold)
[58] Bersuker I B 2001 *Chem. Rev.* **101** 1067
[59] Wojciechowski P M, Zierkiewicz W, Michalska D and Hobza P 2003 *J. Chem. Phys.* **118** 10900